Published in final edited form as:
J Control Release. 2014 July 10; 185: 1–11. doi:10.1016/j.jconrel.2014.03.047.

Hydrodynamic Delivery of FGF21 Gene Alleviates Obesity and Fatty Liver in Mice Fed a High-fat Diet

Mingming Gao, **Yongjie Ma**, **Ran Cui**, and **Dexi Liu***
Department of Pharmaceutical and Biomedical Sciences, College of Pharmacy, University of Georgia, Athens, GA 30602

Abstract

FGF21 is a secreted protein that plays critical roles in regulating glucose and lipid metabolism. In this study, we evaluated the effects of FGF21 gene transfer on C57BL/6 mice fed a high fat diet (HFD). We demonstrate that transfer of the FGF21 gene using a hydrodynamics-based procedure increased mRNA levels of FGF21 exclusively in the liver, consequently generating a sustained high level of FGF21 protein in blood that peaked at 500 ng/ml one day after injection, leading to a variety of beneficial effects including blockade of HFD-induced obesity, alleviation of fatty liver and improvement in glucose homeostasis. These effects were associated with altered expression of *Ucp1*, *Dio2*, *Pgc1α*, *Pparγ2*, *Mgat1*, *F4/80*, *Mcp1* and *Tnfα*, which are involved in thermogenesis, lipogensis and chronic inflammation in the liver and adipose tissues. Transfer of the FGF21 gene in HFD-induced obese mice greatly increased expression of thermogenic genes in adipose tissue, resulting in similar improvements in systemic metabolism including reduction of adiposity, alleviation of fatty liver and attenuation of insulin resistance. Mechanistic studies on the effects of FGF21 gene transfer in lean mice revealed that mice transferred with FGF21 gene displayed suppressed lipogenesis in the liver and enhanced thermogenesis in brown adipose tissue which was coincident with a significant improvement in glucose tolerance. Collectively, our results suggest transfer of the FGF21 gene could be considered a promising approach for treating obesity and its complications.

Keywords

Hydrodynamic gene delivery; FGF21; obesity; diabetes; fatty liver; thermogenesis

*Correspondence: Dexi Liu, PhD, Panoz Professor, Department of Pharmaceutical and Biomedical Sciences, College of Pharmacy, University of Georgia, 450 Pharmacy South, 250 West Green Street, Athens, GA 30602, dliu@uga.edu.

Conflict of Interest
The authors claim no conflicts of interest.

Introduction

Fibroblast growth factor 21 (FGF21) is a member of the fibroblast growth factor family, but unlike many other classical FGFs, FGF21 functions primarily as an endocrine hormone rather than a growth factor regulating cell differentiation and proliferation [1]. Studies have shown that FGF21 is able to generate a variety of beneficial effects in metabolic disorders. For instance, Kharitonenkov *et al* reported FGF21 transgenic mice were resistant to diet-induced obesity, and therapeutic administration of recombinant FGF21 protein greatly reduced plasma glucose and lipids in *ob/ob* mice [2]. On the contrary, FGF21 deficiency led to increased body weight, development of fatty liver, impaired glucose tolerance, and elevated blood insulin [1, 3, 4]. Subsequent studies by Xu *et al* showed FGF21 dose-dependently reduced body weight and improved metabolic homeostasis in diet-induced obese mice, largely through increasing energy expenditure [5, 6]. Mechanistically FGF21 may be a key mediator of pharmacologic actions of PPARα and PPARγ [3, 7, 8]. Moreover, a recent study by Spiegelman *et al* revealed FGF21 plays a physiological role in thermogenic recruitment of white adipose tissue, and mice deficient in FGF21 display an impaired ability to adapt to chronic cold exposure [9]. These actions partly rely on the FGF21-PGC1α-UCP1 axis.

Despite beneficial effects, the FGF21 protein has a short half-life *in vivo* (less than 2 hr in mice) [6], which compromises its potential application in disease treatment. Several approaches, including fusion protein construction [10, 11] and chemical modification [12-14], have been attempted to solve this issue. Although showing early signs of promise, these engineered protein molecules may cause increased immunogenicity and antigenicity, which may result in loss of drug effectiveness [15]. Additionally, since these engineered proteins maybe eliminated within hours or days, multiple repeated injections are required to maintain the therapeutic effects. These limitations make it necessary to develop new approaches to apply FGF21 in treating metabolic disorders. As an alternative and more cost-effective approach, FGF21 gene transfer may be able to generate a sustained high level of circulating FGF21 which consequently leads to similar beneficial effects in metabolism.

In this study, we evaluated the effects of FGF21 gene transfer using hydrodynamic tail vein injection in C57BL/6 mice fed a high-fat diet (HFD), and investigated its underlying mechanism. Our data clearly shows FGF21 gene transfer produced a persistent high level of FGF21 in circulation, leading to a blockade of HFD-induced obesity, insulin resistance and fatty liver, which were associated with increased expression of genes involved in adaptive thermogenesis in adipose tissue. In diet-induced obese mice, FGF21 gene transfer reduced adiposity, improved glucose intolerance and alleviated fatty liver. Our results suggest hydrodynamic transfer of the FGF21 gene can be considered a potential strategy for treating obesity as well as its complications such as insulin resistance and fatty liver.

Materials and Methods

The pLIVE plasmid vector was purchased from Mirus Bio (Madison, WI), and the mouse FGF21 gene was cloned from complementary DNA sequences of C57BL/6 mice using high-fidelity DNA polymerase purchased from NEB (Ipswich, MA). The FGF21 gene was

inserted into multi-cloning sites of the pLIVE vector using restriction enzyme digestion, and thereafter confirmed using DNA sequencing. The same vector with green fluorescence protein (GFP) gene was constructed using the same procedure. These plasmids were purified using cesium chloride-ethidium bromide gradient centrifugation and kept in saline at −80 °C until use. Optical density determination (260 and 280 nm) and 1% agarose gel electrophoresis were performed to examine the purity of the plasmid preparations.

Animals and treatments

Male C57BL/6 mice purchased from Charles River Laboratories (Wilmington, MA) were housed under standard conditions with a 12-hr light-dark cycle. All procedures performed on animals were approved by the Institutional Animal Care and Use Committee at the University of Georgia, Athens, Georgia (protocol number, A2011 07-Y2-A3). HFD (60% kJ/fat, 20% kJ/carbohydrate, 20% kJ/protein) used in this study was purchased from Bio-Serv (Frenchtown, NJ; #F3282). The procedure for standard hydrodynamic tail vein injection in mice has previously been reported [16, 17]. Briefly, saline solution equal to 9% body weight containing 20 μg plasmid DNA was injected into a mouse tail vein within 5-8 seconds. The adjusted hydrodynamic injection in obese mice was performed according to lean mass. Briefly, 2.0-2.5 ml saline solution (equivalent to 8% lean mass of obese mice) containing 20 μg plasmid DNA was injected into the tail vein of each of the obese mice within 5-8 seconds.

Experimental design

In the experiment aimed confirming gene expression and protein production, two groups of mice (~22 g, n=5 for each group) were injected with plasmid DNA containing GFP or the FGF21 gene. Mice were euthanized using CO_2 three days after plasmid injection for assessment of mRNA and protein level. The acute effects of FGF21 gene transfer were studied in a period of 7 days after hydrodynamic gene delivery. The prevention of HFD-induced obesity was conducted on mice with starting body weight at ~30 g (n=5). The treatment study was carried out in HFD-induced obese mice (~52 g, n=5) using adjusted hydrodynamic procedure. Body weight and food intake were measured weekly, and body composition analysis was performed at the conclusion of the experiment using EchoMRI-100 (Echo Medical Systems, Houston, TX). Animals in the control group were injected with plasmid DNA containing GFP gene and those in the other group with plasmid DNA containing FGF21 gene.

Examination of FGF21 protein level in blood

Blood samples were collected from mouse tail veins using Microvette-CB300-LH (#22-043975) purchased from Fisher Scientific (Pittsburgh, PA). Plasma was isolated by centrifugation at 4,000 rpm for 5 minutes, and kept at -80 °C until use. Circulating FGF21 was measured using an enzyme-linked immunosorbent assay (ELISA) kit purchased from Aviscera Bioscience (#SK00145-08, Santa Clara, CA), and ELISA was conducted following a protocol provided by the manufacture.

Examination of FGF21 mRNA level in hydrodynamically transfected mice

Total RNA was isolated from the mouse liver and white and brown adipose tissue using an RNeasy kit (#74804) purchased from QIAGEN (Valencia, CA). One μg of total RNA were used for the first strand cDNA synthesis using a Superscript RT III enzyme kit (#11752-050) from Invitrogen. Quantitative real-time PCR (qPCR) was conducted using SYBR Green as the detection reagent on the ABI StepOnePlus Real-Time PCR system. The data were analyzed using the ΔΔCt method [18] and normalized to internal control of GAPDH mRNA. Primers were synthesized at Sigma (St. Louis, MO). All primer sequences employed are summarized in Supplementary Table 1. Melting curve analysis of all real-time PCR products was conducted and showed a single DNA duplex.

Evaluation of glucose homeostasis

An intraperitoneal glucose tolerance test (IPGTT) was carried out in mice fasted for six hr. Glucose solubilized in phosphate-buffered saline was injected (*i.p.*) at 2 g/kg, and the time-point was set as 0 min. Blood glucose was measured at predetermined time-points (0, 30, 60, and 120 minutes) using glucose test strips and glucose meters. Intraperitoneal insulin tolerance test (ITT) was performed in mice fasted for four hr. Insulin (Humulin, 0.75 U/kg) purchased from Eli Lilly (Indianapolis, IN) was injected (*i.p.*), and blood glucose was measured at predetermined time-points identical to IPGTT. Blood insulin was measured using an ELISA kit (#10-1113-01) purchased from Mercodia Developing Diagnostics (Winston Salem, NC). HOMA-IR was calculated using the following formula as described before [19]: HOMA-IR = (fasting insulin (ng/ml) × fasting plasma glucose (mg/dl)/405).

Histochemical and immunohistochemical examination

For histochemical examination using haematoxylin and eosin (H&E) staining, liver samples were embedded into paraffin and cut at 6 μm in thickness. Staining was performed using a commercial kit (#3500, BBC Biochemical, Atlanta, GA). Size measurement of adipocytes was conducted under an optical microscope (ECLIPSE Ti, Nikon) using an NIS-Elements imaging platform purchased from Nikon Instruments Inc. (Melville, NY). For Oil-red O staining and Nile red staining, liver samples were frozen in liquid nitrogen and sectioned at 8 μm in thickness using a Cryostat. These sections were stained using Oil-red O (Electron Microscopy Sciences, Hatfield, PA) for 30 min (counterstained using haematoxylin) or Nile red (Sigma, St. Louis, MO) for 5 min (counterstained using DAPI). Immunohistochemical (IHC) staining was carried out using an FGF21 antibody (#sc-16842) purchased from Santa Cruz Biotechnology (Santa Cruz, CA) and a staining kit (#DAB150) purchased from Millipore (Billerica, MA).

Determination of liver triglyceride

The procedure for quantitative determination of liver triglyceride has been previously described [20]. Liver samples (200-400 mg) were homogenized in a mixture of chloroform and methanol (2:1, volume ratio), and thereafter incubated overnight at 4°C. The tissue homogenates were centrifuged at 12,000 rpm for 20 min, and the supernatants were dried and re-dissolved in 5% Triton-X100. The triglyceride concentration was determined using a commercial kit (#TR22203, Thermo-Scientific).

Statistics

Statistical analysis was performed using the Student's *t* test, and all results were expressed as the mean ± SD. A *P* value below 0.05 ($P < 0.05$) was considered significantly different.

Results

Hydrodynamic transfer of FGF21 gene increased mRNA level in the liver and protein levels of FGF21 in the circulation

Mice transferred with the FGF21 gene showed a markedly increased FGF21 mRNA level in the liver as measured by reverse-transcription PCR 3 days after hydrodynamic injection (Figure 1A). Hydrodynamic injection of FGF21 gene increased FGF 21 mRNA levels by ~364-fold exclusively in the liver (Figure 1B) but not in other organs such as the heart, spleen, lung and kidney, confirming the liver specificity of the procedure. Strong green fluorescence signals were observed in the liver and collected from mice transferred with the GFP gene but not the FGF21 gene (Figure 1C). On the contrary, positive signals of FGF21 IHC staining were seen in livers transferred with the FGF21 gene but not in those transferred with the GFP gene (Figure 1C). Hydrodynamic injection of the FGF21 gene generated a sustained high level of circulating FGF21 which reached ~500 ng/ml one day after injection and gradually decreased thereafter (Figure 1D).

FGF21 gene transfer blocked HFD-induced obesity and enlargement of adipocytes

Control mice that received the GFP gene showed an average rate of body weight gain at ~1.7 g/week, while that of mice with FGF21 gene was ~0.5 g/week (Figure 2A). Eventually, the difference in the body weight between two groups was ~8.3 g (Figure 2A) which can be easily recognized by the naked eye (Figure 2B). No significant difference was observed in average food intake between control and treated groups (Figure 2C). Body composition analysis showed that the difference in body weight gain was predominantly in fat mass, not lean mass (Figure 2D). Measurement of the weight of fat pads showed significant difference in epididymal white adipose tissue (EWAT), perirenal white adipose tissue (PWAT) and inguinal (IWAT) between control and FGF21 groups (Figure 2E). H&E staining (Figure 2F) showed FGF21 gene transfer greatly suppressed the HFD-induced enlargement of adipocytes in EWAT, PWAT and IWAT, and a higher density of the cellular matrix in BAT of treated mice compared to that of control mice. Quantification using the image system showed the same conclusion (Figure 2G).

FGF21 gene transfer protected mice from HFD-induced fatty liver

Mice with the FGF21 gene transfer had a lower liver weight compared with that of control mice (Figure 3A). Gross imaging showed the FGF21 gene transfer suppressed HFD-induced enlargement of the liver (Figure 3B). H&E staining showed more vacuoles in the control liver compared to that transferred with the FGF21 gene (Figure 3B). The red dots in Oil-red O staining and Nile red staining confirmed these vacuoles were lipid droplets (Figure 3B). Biochemical quantitative determination further verified that the FGF21 gene transfer repressed HFD-induced triglyceride (TG) deposition in the liver (Figure 3C). No significant change occurred in blood AST and ALT (Figure 3D). Gene expression analysis showed

FGF21 gene transfer markedly repressed transcription of key genes involved in lipid metabolism, including *Pparγ2* (~51%), *Cd36* (~72%), *Fabp4* (~53%) and *Mgat1* (~85%) (Figure 3E). On the contrary, transfer of the FGF21 gene slightly, but significantly, increased expression of genes for fatty acid *β* oxidation such as *Cpt1a* (~2.2-folds) and *Acadl* (~1.8-fold) (Figure 3F). Additionally, FGF21 gene transfer slightly suppressed expression of *Scd1* (~45%) (Figure 3G).

FGF21 gene transfer prevented HFD-induced insulin resistance and glucose intolerance

Mice transferred with the FGF21 gene showed a decreased fasting glucose compared to control mice (Figure 4A). IPGTT showed FGF21 gene transfer greatly suppressed the elevation of the glucose profile induced by injection of glucose saline, demonstrating that these mice possessed improved glucose tolerance (Figure 4B). Calculation of the AUC provided the same conclusion confirming FGF21 gene transfer repressed the AUC of IPGTT by ~40% (Figure 4C). Blood insulin levels for control and treated mice were ~4.1 ng/ml and ~1.9 ng/ml, respectively (Figure 4D). Compared to control, mice transferred with the FGF21 gene showed larger decreases in their glucose profiles in response to insulin injections, indicating improved insulin sensitivity in these mice (Figure 4E). Calculation of the HOMA-IR offered the same conclusion (Figure 4F). No significant difference was observed in H&E staining of the islets between the two groups (Figure 4G).

Suppressed body weight gain was associated with altered gene expression in adipose tissues

FGF21 gene transfer markedly suppressed expression of genes involved in chronic inflammation of adipose tissue including *Mcp1* (~92%), *Tnfα* (~76%), *Ifnγ* (~40%), *Il1β* (~85%) and *Il6* (~81%) (Figure 5A). Expression of macrophage marker genes such as *F4/80* (~79%), *Cd11b* (~80%) and *Cd11c* (~95%) were also greatly decreased in mice transferred with the FGF21 gene (Figure 5B). Additionally, mice transferred with the FGF21 gene showed decreased mRNA levels of *Leptin* (~75%) and *Fgf21* (~67%) in adipose tissue (Figure 5C). On the contrary, all genes involved in adaptive thermogenesis including *Ucp1* (~47.2-folds), *Ucp2* (~2.4-folds), *Ucp3* (~1.7-fold), *Dio2* (~1.6-fold), *Pgc1α* (~1.9-fold), *Cidea* (~2.8-folds) and *Elovl3* (~29.3-folds) showed significant increase in the IWAT of mice transferred with the FGF21 gene (Figure 5D). Similar changes were observed in the BAT of mice transferred with the FGF21 gene (Figure 5E).

Hydrodynamic gene transfer to HFD-induced obese mice

The relation between body weight and fat mass, and body weight and lean mass in HFD-induced obese mice with a body weight of 40-55 g was analyzed and plotted. As expected, these obese mice had a high ratio of fat mass (28%-47% of body weight) (Figure 6A). Fat mass increased at a rate of 0.64 g/g body weight while lean mass increased at a much lower rate of 0.30 g/g body weight, suggesting the fat mass provided a larger contribution to the increase in body weight in obese mice (Figure 6A and Figure 6B). With these findings, we adjusted the hydrodynamic procedure, and calculated the saline volume based on lean mass rather than total body weight. Although weaker than that of lean mice, the GFP signals in obese mice using the adjusted procedure (8% lean mass as the injection volume) is still

easily recognized (Figure 6C). Additionally, hydrodynamic injection in obese mice using the adjusted procedure did not affect the gross morphology and lipid droplets in the liver (Figure 6C).

FGF21 gene transfer decreased body weight and reduced adipocyte size in HFD-induced obese mice

We measured mRNA and protein levels of FGF21 in obese mice two weeks after injection and found hydrodynamic injection of FGF21 gene markedly increased mRNA level of FGF21 in the liver (~17-folds), and consequently elevated circulating FGF21 in the serum (~40-folds) (Supplementary Figures 1A-B). No significant change was observed in AST and ALT at the end of the experiment (Supplementary Figure 1C). As expected, hydrodynamic transfer of the FGF21 gene greatly decreased the body weight of obese mice by ~7.8 g within two weeks, while control mice receiving the GFP gene did not show a significant change in body weight (Figure 7A and Figure 7B). No significant difference was observed in average food intake between the two groups (Figure 7C). Determination of body composition showed the decrease in body weight was mainly derived from fat mass, not lean mass (Figure 7D). Mice receiving the FGF21 gene showed reduced fat pad weight at EWAT (~0.9 g), PWAT (~0.6 g) and IWAT (~1.0 g) (Figure 7E). H&E staining showed FGF21 gene transfer greatly suppressed the size of adipocytes in EWAT, PWAT and IWAT (Figure 7F). The same conclusion was provided by quantification using an imaging system (Figure 7G). Surprisingly, mice transferred with the FGF21 gene showed a significantly higher density of the cellular matrix in BAT compared to that of control (Figure 7F).

FGF21 gene transfer alleviated fatty liver in HFD-induced obese mice

Transfer of the FGF21 gene in obese mice greatly decreased liver weight and reduced its size (Figure 8A and Figure 8B). H&E staining showed the total amount of vacuoles was markedly reduced by FGF21 gene transfer (Figure 8B). Consistently, Oil-red O staining and Nile red staining showed less red dots in the liver of mice receiving the FGF21 gene (Figure 8B), suggesting the severity of fatty liver had been alleviated in these mice. This conclusion was further confirmed by biochemical quantification showing TG levels were ~72 and ~31 mg/g tissue in mice receiving the GFP gene and FGF21 gene, respectively (Figure 8C). Gene expression analysis showed the transcription of multiple genes involved in lipids and glucose metabolism was significantly reduced in the liver of obese mice transferred with the FGF21 gene, including *Pparγ2* (~65%), *Cd36* (~47%), *Fabp4* (~32%), *Mgat1* (~77%), Fas (~65%), *Scd1* (~95%) and *G6p* (~44%) (Figure 8D).

FGF21 gene transfer in HFD-induced obese mice altered gene expression in adipose tissues and improved glucose metabolism

We determined the expression of genes involved in adaptive thermogenesis in IWAT, and found most of them markedly increased in obese mice transferred with the FGF21 gene, including *Ucp1* (~36.6-folds), *Ucp3* (~2.1-folds), *Dio2* (~3.6-folds), *Pgc1α* (~2.0-folds), *Cidea* (~6.4-folds) and *Elovl3* (~21.7-folds) (Figure 9A). Similar changes were observed in BAT of these mice (Figure 9B). FGF21 gene transfer greatly repressed elevation of glucose profile in IPGTT (Figure 9C). Calculation of the AUC provided the same conclusion (Figure

9D). Blood insulin was ~5.5 ng/ml and ~3.0 ng/ml for control and treated mice, respectively (Figure 9E). Consistently, mice receiving the FGF21 gene showed higher insulin sensitivity in ITT (Figure 9F). No significant change was observed between two groups in H&E staining of the pancreatic islets (Figure 9G).

Effects of FGF21 gene transfer on lean mice

Next, we investigated the effects of FGF21 gene transfer on lean mice. Mice receiving the FGF21 gene showed a reduction in the size of adipocytes in IWAT and a higher density of cellular matrix in BAT without a significant change in liver (Figure 10A). IPGTT and the following AUC calculation demonstrated FGF21 gene transfer improved glucose tolerance even in lean mice (Figure 10B and Figure 10C). Gene expression analysis of liver samples showed FGF21 gene transfer markedly reduced transcription of key genes involved in lipogenesis, such as *Pparγ2* (~63%), *Fabp4* (~48%), *Mgat1* (~97%), *Srebp1c* (~59%) and *fas* (~61%) (Figure 10D). On the contrary, the expression of multiple thermogenic genes was greatly increased in BAT of mice receiving FGF21 gene, such as *Ucp1* (~2.5-folds), *Dio2* (~5.0-folds), *Pgc1α* (~2.8-folds) and *Elovl3* (~7.5-folds) (Figure 10E).

Discussion

In this study, we demonstrated that FGF21 gene transfer by hydrodynamic tail vein injection generated a sustained high level of circulating FGF21 (Figure 1), leading to a blockade of HFD-induced obesity (Figure 2) and fatty liver (Figure 3) and glucose intolerance (Figure 4). These beneficial effects were associated with increased expression of genes for adaptive thermogenesis and suppressed expression of genes involved in chronic inflammation in adipose tissues (Figure 5). HFD-induced obese mice transferred with the FGF21 gene using adjusted hydrodynamic injection (Figure 6) showed decreased adiposity (Figure 7), alleviated fatty liver (Figure 8), increased expression of genes for thermogenesis and improved glucose homeostasis (Figure 9). Mechanistic studies on the acute effects of FGF21 gene transfer revealed that FGF21 modulated transcription of a variety of genes involved in lipogenesis and thermogenesis in liver and brown adipose tissue, resulting in an improvement in glucose tolerance even in lean mice (Figure 10).

The suppressive effect of FGF21 gene transfer on adiposity can be attributed to its action in elevating expression of genes for thermogenesis. Accumulating evidence suggests FGF21 is actively involved in adaptive thermogenesis which is critical to maintain the homeostasis of body temperature. For example, a previous study by Hondares *et al* using neonatal mice demonstrated that FGF21 produced by the liver increased expression of thermogenic genes within BAT, leading to activation of BAT thermogenesis [21]. Subsequent studies by Hondares *et al* and Chartoumpekis *et al* consistently demonstrates that in response to thermogenic activation by cold exposure or β3-adrenergic stimulation, BAT becomes a source of systemic FGF21, further enhancing BAT thermogenesis in an autocrine manner [22, 23]. Consistent with these previous reports, in this study, we observed that FGF21 gene transfer greatly increased expression of multiple genes critical for thermogenesis in BAT such as *Ucp1*, *Dio2*, *Pgc1α* and *Elovl3* (Figure 5E, Figure 9B and Figure 10E). In addition to BAT, white adipose tissue may also be targets of FGF21 for thermogenesis. The initial

study completed by Spiegelman and colleagues provided convincing evidence that FGF21 is able to regulate PGC1α and browning of white adipose tissue [9]. Following studies by Lee *et al* and Kim *et al* prove that FGF21 derived from beige cells and muscle is capable of promoting a brown fat-like thermogenic program in white adipocytes and elevating energy expenditure [24, 25]. In line with these above studies, our data showed that mice receiving the FGF21 gene exhibited significant increase in transcription of thermogenic genes in WAT including *Ucp1*, *Dio2*, *Pgc1α*, *Cidea* and *Elovl3* (Figure 5D and Figure 9A), indicating an enhanced thermogenesis may occur in this tissue. Due to these facts, we believe that FGF21 gene transfer negatively regulated adiposity, at least in part, through increasing thermogenesis in adipose tissue.

FGF21 plays important roles in maintaining glucose homeostasis by regulating glucose uptake in peripheral tissues as well as stimulating signal pathways in pancreatic β cells. Previous studies by Kharitonenkov *et al* demonstrate that FGF21 stimulates glucose uptake in adipocytes by increasing GLUT1 expression, and systemic administration of FGF21 reduced plasma glucose to near normal levels in diabetic rodents as well as nonhuman primates [2, 26]. Xu *et al* provided compelling evidence showing FGF21 is able to reduce blood glucose and insulin in diet-induced obese mice, and the improvement of insulin resistance is independent of reduction in body weight and adiposity [5]. Moreover, Wente *et al* demonstrates that FGF21 protected pancreatic β cells from glucolipotoxicity and cytokine-induced apoptosis via the Erk1/2 and Akt signaling pathways [27]. In line with these previous reports, our data clearly show that FGF21 gene transfer significantly reduced hyperinsulinemia and attenuated insulin resistance in mice fed a HFD, consequently leading to significant improvements in glucose tolerance (Figure 4 and Figure 9). Interestingly, we also observed an acute effect of FGF21 gene transfer in glucose homeostasis in lean mice (Figure 10) which was consistent with a very recent study by Shulman and colleagues showing that infusion of FGF21 was able to improve insulin responsiveness in regular chow-fed wild-type mice [28]. The acute effect may be explained by the insulin-independent activity of FGF21 in enhancing glucose uptake in muscle and adipose tissue [29, 30]. In addition, mounting evidence suggests that macrophage infiltration and chronic inflammation in adipose tissue is positively correlated with insulin resistance and glucose intolerance [31-33]. Therefore, in this study, we measured expression of their marker genes, and found that all were greatly repressed in the adipose tissue of mice receiving FGF21 gene (Figure 5A-B). Suppressed chronic inflammation may also contribute to improved glucose tolerance. However, the possibility that FGF21 may improve glucose tolerance through its effects on the central nervous system cannot be excluded [34].

Previous studies have identified FGF21 as a key regulator for enhancing lipid oxidation and suppressing *de novo* lipogenesis. Using diet-induced obese mice and *ob*/*ob* mice as animal models, Coskun *et al* demonstrated that FGF21 was able to increase fat utilization, energy expenditure and futile cycling in adipose tissue, leading to profound improvement in fatty liver [35]. Similarly, Xu *et al* demonstrated that daily injections of FGF21 inhibited SREBP1 and suppressed the expression of a wide array of genes involved in fatty acid and triglyceride synthesis, resulting in a dramatic reduction in hepatic triglyceride levels [5]. Consistent with these findings, we observed an acute effect of FGF21 gene transfer on the

liver of lean mice showing markedly repressed expression of multiple genes involved in lipogenesis including *Pparγ2*, *Fabp4*, *Mgat1*, *Srebp1c* and *Fas* (Figure 10D). Moreover, FGF21 gene transfer in mice fed a HFD greatly suppressed transcription of several key genes for lipogenesis in liver, leading to a corresponding alleviation of fatty liver (Figure 3 and Figure 8).

FGF21 possesses potent activity in inducing energy expenditure, increasing glucose uptake, enhancing lipids oxidation as well as suppressing triglyceride synthesis, consequently producing profound improvements in systemic metabolism [36]. Due to the capability of generating a variety of beneficial effects in metabolism, FGF21 has attracted considerable interest as a potential therapeutic agent in treating obesity and its complications [36, 37]. Despite these beneficial effects, the application of FGF21 in clinic is limited by its short half-life which is less than 2 hours in mice [6]. Multiple approaches have been attempted to solve this issue. For example, several studies report that polyethylene glycol (PEG) conjugation largely prolongs the bioactivity of FGF21 *in vivo* with an acceptable level of vacuole formation rate in the kidney which was a common risk associated with PEG conjugation [12-14]. Hecht R *et al* constructed a fusion protein consisting of a mutated FGF21 (L98R, P171G) and the Fc region of human immunoglobulin IgG1, which prolonged the half-life of native FGF21 from 1-2 to 11 hr for Fc-FGF21 in mice [10]. Although displaying prolonged half-life *in vivo*, these engineered proteins still require multiple repeated injections to maintain the therapeutic effects. In this study, FGF21 gene transfer via hydrodynamic injection generated a persistent high level of circulating FGF21 (Figure 1), leading to similar levels of improvements in metabolic disorders induced by HFD feeding, showing great promise for potential clinical application. Meanwhile, since potential toxicity of FGF21 in skeletal homeostasis has been indicated in previous studies [38-40], additional studies are needed to examine whether the gene therapy approach employed in this study will result in the same effect. Further study is needed to establish the relationship between skeletal homeostasis and the level and duration of FGF21 expression. Similarly, an investigation to explore how FGF21 leads to bone loss and the new strategies to block the side effect is desirable.

In summary, in this study, we demonstrate that hydrodynamic transfer of the FGF21 gene can generate multiple beneficial effects in metabolic disorders, including reduction of adiposity, alleviation of fatty liver and improvement of insulin resistance. Our data strongly suggest that transfer of the FGF21 gene using hydrodynamic injection could be an effective approach for treating obesity and its complications which affects approximately 35% Americans.

Supplementary Material

Refer to Web version on PubMed Central for supplementary material.

Acknowledgments

The study was supported in part by grants from NIH (RO1EB007357 and RO1HL098295). We thank Ms. Ryan Fugett for English editing.

References

1. Kharitonenkov A. FGFs and metabolism. Curr Opin Pharmacol. 2009; 9:805–810. [PubMed: 19683963]
2. Kharitonenkov A, Shiyanova TL, Koester A, Ford AM, Micanovic R, Galbreath EJ, Sandusky GE, Hammond LJ, Moyers JS, Owens RA, Gromada J, Brozinick JT, Hawkins ED, Wroblewski VJ, Li DS, Mehrbod F, Jaskunas SR, Shanafelt AB. FGF-21 as a novel metabolic regulator. J Clin Invest. 2005; 115:1627–1635. [PubMed: 15902306]
3. Badman MK, Pissios P, Kennedy AR, Koukos G, Flier JS, Maratos-Flier E. Hepatic fibroblast growth factor 21 is regulated by PPARalpha and is a key mediator of hepatic lipid metabolism in ketotic states. Cell Metab. 2007; 5:426–437. [PubMed: 17550778]
4. Kharitonenkov A, Shanafelt AB. FGF21: a novel prospect for the treatment of metabolic diseases. Curr Opin Investig Drugs. 2009; 10:359–364.
5. Xu J, Lloyd DJ, Hale C, Stanislaus S, Chen M, Sivits G, Vonderfecht S, Hecht R, Li YS, Lindberg RA, Chen JL, Jung DY, Zhang Z, Ko HJ, Kim JK, Veniant MM. Fibroblast growth factor 21 reverses hepatic steatosis, increases energy expenditure, and improves insulin sensitivity in diet-induced obese mice. Diabetes. 2009; 58:250–259. [PubMed: 18840786]
6. Xu J, Stanislaus S, Chinookoswong N, Lau YY, Hager T, Patel J, Ge H, Weiszmann J, Lu SC, Graham M, Busby J, Hecht R, Li YS, Li Y, Lindberg R, Veniant MM. Acute glucose-lowering and insulin-sensitizing action of FGF21 in insulin-resistant mouse models--association with liver and adipose tissue effects. Am J Physiol Endocrinol Metab. 2009; 297:E1105–1114. [PubMed: 19706786]
7. Gao M, Bu L, Ma Y, Liu D. Concurrent activation of liver X receptor and peroxisome proliferator-activated receptor alpha exacerbates hepatic steatosis in high fat diet-induced obese mice. PLoS One. 2013; 8:e65641. [PubMed: 23762402]
8. Dutchak PA, Katafuchi T, Bookout AL, Choi JH, Yu RT, Mangelsdorf DJ, Kliewer SA. Fibroblast growth factor-21 regulates PPARgamma activity and the antidiabetic actions of thiazolidinediones. Cell. 2012; 148:556–567. [PubMed: 22304921]
9. Fisher FM, Kleiner S, Douris N, Fox EC, Mepani RJ, Verdeguer F, Wu J, Kharitonenkov A, Flier JS, Maratos-Flier E, Spiegelman BM. FGF21 regulates PGC-1alpha and browning of white adipose tissues in adaptive thermogenesis. Genes Dev. 2012; 26:271–281. [PubMed: 22302939]
10. Hecht R, Li YS, Sun J, Belouski E, Hall M, Hager T, Yie J, Wang W, Winters D, Smith S, Spahr C, Tam LT, Shen Z, Stanislaus S, Chinookoswong N, Lau Y, Sickmier A, Michaels ML, Boone T, Veniant MM, Xu J. Rationale-based engineering of a potent long-acting FGF21 analog for the treatment of type 2 diabetes. PLoS One. 2012; 7:e49345. [PubMed: 23209571]
11. Smith R, Duguay A, Weiszmann J, Stanislaus S, Belouski E, Cai L, Yie J, Xu J, Gupte J, Wu X, Li Y. A novel approach to improve the function of FGF21. BioDrugs. 2013; 27:159–166. [PubMed: 23456652]
12. Huang Z, Wang H, Lu M, Sun C, Wu X, Tan Y, Ye C, Zhu G, Wang X, Cai L, Li X. A better anti-diabetic recombinant human fibroblast growth factor 21 (rhFGF21) modified with polyethylene glycol. PLoS One. 2011; 6:e20669. [PubMed: 21673953]
13. Mu J, Pinkstaff J, Li Z, Skidmore L, Li N, Myler H, Dallas-Yang Q, Putnam AM, Yao J, Bussell S, Wu M, Norman TC, Rodriguez CG, Kimmel B, Metzger JM, Manibusan A, Lee D, Zaller DM, Zhang BB, DiMarchi RD, Berger JP, Axelrod DW. FGF21 analogs of sustained action enabled by orthogonal biosynthesis demonstrate enhanced antidiabetic pharmacology in rodents. Diabetes. 2012; 61:505–512. [PubMed: 22210323]
14. Xu J, Bussiere J, Yie J, Sickmier A, An P, Belouski E, Stanislaus S, Walker KW. Polyethylene glycol modified FGF21 engineered to maximize potency and minimize vacuole formation. Bioconjug Chem. 2013; 24:915–925. [PubMed: 23594041]
15. Schellekens H. Immunogenicity of therapeutic proteins: clinical implications and future prospects. Clin Ther. 2002; 24:1720–1740. discussion 1719. [PubMed: 12501870]
16. Liu F, Song Y, Liu D. Hydrodynamics-based transfection in animals by systemic administration of plasmid DNA. Gene Ther. 1999; 6:1258–1266. [PubMed: 10455434]

17. Zhang G, Budker V, Wolff JA. High levels of foreign gene expression in hepatocytes after tail vein injections of naked plasmid DNA. Hum Gene Ther. 1999; 10:1735–1737. [PubMed: 10428218]
18. Livak KJ, Schmittgen TD. Schmittgen, Analysis of relative gene expression data using realtime quantitative PCR and the 2(-Delta Delta C(T)) Method. Methods. 2001; 25:402–408. [PubMed: 11846609]
19. Gao M, Zhang C, Ma Y, Bu L, Yan L, Liu D. Hydrodynamic delivery of mIL10 gene protects mice from high-fat diet-induced obesity and glucose intolerance. Mol Ther. 2013; 21:1852–1861. [PubMed: 23774795]
20. Gao M, Liu D. Resveratrol suppresses T0901317-induced hepatic fat accumulation in mice. AAPS J. 2013; 15:744–752. [PubMed: 23591747]
21. Hondares E, Rosell M, Gonzalez FJ, Giralt M, Iglesias R, Villarroya F. Hepatic FGF21 expression is induced at birth via PPARalpha in response to milk intake and contributes to thermogenic activation of neonatal brown fat. Cell Metab. 2010; 11:206–212. [PubMed: 20197053]
22. Hondares E, Iglesias R, Giralt A, Gonzalez FJ, Giralt M, Mampel T, Villarroya F. Thermogenic activation induces FGF21 expression and release in brown adipose tissue. J Biol Chem. 2011; 286:12983–12990. [PubMed: 21317437]
23. Chartoumpekis DV, Habeos IG, Ziros PG, Psyrogiannis AI, Kyriazopoulou VE, Papavassiliou AG. Brown adipose tissue responds to cold and adrenergic stimulation by induction of FGF21. Mol Med. 2011; 17:736–740. [PubMed: 21373720]
24. Lee P, Werner CD, Kebebew E, Celi FS. Functional thermogenic beige adipogenesis is inducible in human neck fat. Int J Obes (Lond). 2013 Epub ahead of print. 10.1038/ijo.2013.82
25. Kim KH, Jeong YT, Oh H, Kim SH, Cho JM, Kim YN, Kim SS, Kim do H, Hur KY, Kim HK, Ko T, Han J, Kim HL, Kim J, Back SH, Komatsu M, Chen H, Chan DC, Konishi M, Itoh N, Choi CS, Lee MS. Autophagy deficiency leads to protection from obesity and insulin resistance by inducing Fgf21 as a mitokine. Nat Med. 2013; 19:83–92. [PubMed: 23202295]
26. Kharitonenkov A, Wroblewski VJ, Koester A, Chen YF, Clutinger CK, Tigno XT, Hansen BC, Shanafelt AB, Etgen GJ. The metabolic state of diabetic monkeys is regulated by fibroblast growth factor-21. Endocrinology. 2007; 148:774–781. [PubMed: 17068132]
27. Wente W, Efanov AM, Brenner M, Kharitonenkov A, Koster A, Sandusky GE, Sewing S, Treinies I, Zitzer H, Gromada J. Fibroblast growth factor-21 improves pancreatic beta-cell function and survival by activation of extracellular signal-regulated kinase 1/2 and Akt signaling pathways. Diabetes. 2006; 55:2470–2478. [PubMed: 16936195]
28. Camporez JP, Jornayvaz FR, Petersen MC, Pesta D, Guigni BA, Serr J, Zhang D, Kahn M, Samuel VT, Jurczak MJ, Shulman GI. Cellular mechanisms by which FGF21 improves insulin sensitivity in male mice. Endocrinology. 2013; 154:3099–3109. [PubMed: 23766126]
29. Mashili FL, Austin RL, Deshmukh AS, Fritz T, Caidahl K, Bergdahl K, Zierath JR, Chibalin AV, Moller DE, Kharitonenkov A, Krook A. Direct effects of FGF21 on glucose uptake in human skeletal muscle: implications for type 2 diabetes and obesity. Diabetes Metab Res Rev. 2011; 27:286–297. [PubMed: 21309058]
30. Moyers JS, Shiyanova TL, Mehrbod F, Dunbar JD, Noblitt TW, Otto KA, Reifel-Miller A, Kharitonenkov A. Molecular determinants of FGF-21 activity-synergy and cross-talk with PPARgamma signaling. J Cell Physiol. 2007; 210:1–6. [PubMed: 17063460]
31. Weisberg SP, McCann D, Desai M, Rosenbaum M, Leibel RL, Ferrante AW Jr. Obesity is associated with macrophage accumulation in adipose tissue. J Clin Invest. 2003; 112:1796–1808. [PubMed: 14679176]
32. Xu H, Barnes GT, Yang Q, Tan G, Yang D, Chou CJ, Sole J, Nichols A, Ross JS, Tartaglia LA, Chen H. Chronic inflammation in fat plays a crucial role in the development of obesity-related insulin resistance. J Clin Invest. 2003; 112:1821–1830. [PubMed: 14679177]
33. Gao M, Ma Y, Liu D. Rutin suppresses palmitic acids-triggered inflammation in macrophages and blocks high fat diet-induced obesity and fatty liver in mice. Pharm Res. 2013; 30:2940–2950. [PubMed: 23783345]
34. Sarruf DA, Thaler JP, Morton GJ, German J, Fischer JD, Ogimoto K, Schwartz MW. Fibroblast growth factor 21 action in the brain increases energy expenditure and insulin sensitivity in obese rats. Diabetes. 2010; 59:1817–1824. [PubMed: 20357365]

35. Coskun T, Bina HA, Schneider MA, Dunbar JD, Hu CC, Chen Y, Moller A, Kharitonenkov A. Fibroblast growth factor 21 corrects obesity in mice. Endocrinology. 2008; 149:6018–6027. [PubMed: 18687777]

36. Zhang J, Li Y. Fibroblast growth factor 21, the endocrine FGF pathway and novel treatments for metabolic syndrome. Drug Discov Today. 2013 Epub ahead of print. 10.1016/j.drudis.2013.10.021

37. Kharitonenkov A, Shanafelt AB. Fibroblast growth factor-21 as a therapeutic agent for metabolic diseases. BioDrugs. 2008; 22:37–44. [PubMed: 18215089]

38. Wei W, Dutchak PA, Wang X, Ding X, Bookout AL, Goetz R, Mohammadi M, Gerard RD, Dechow PC, Mangelsdorf DJ, Kliewer SA, Wan Y. Fibroblast growth factor 21 promotes bone loss by potentiating the effects of peroxisome proliferator-activated receptor gamma. Proc Natl Acad Sci U S A. 2012; 109:3143–3148. [PubMed: 22315431]

39. Wu S, Levenson A, Kharitonenkov A, De Luca F. Fibroblast growth factor 21 (FGF21) inhibits chondrocyte function and growth hormone action directly at the growth plate. J Biol Chem. 2012; 287:26060–26067. [PubMed: 22696219]

40. Wan Y. Bone marrow mesenchymal stem cells: fat on and blast off by FGF21. Int J Biochem Cell Biol. 2013; 45:546–549. [PubMed: 23270727]

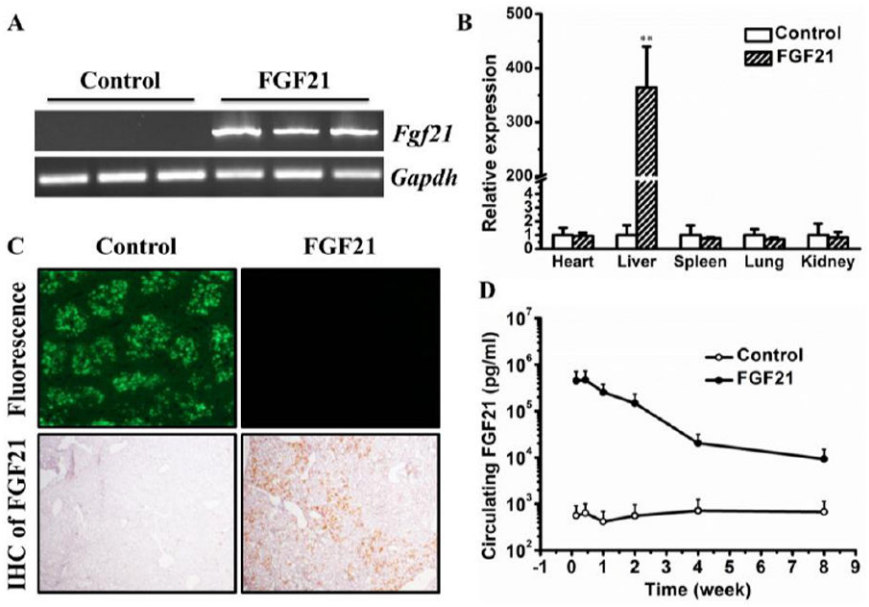

Figure 1. Hydrodynamic tail veil injection of plasmid DNA containing FGF21 gene increased FGF21 mRNA levels in the liver, and generated a sustained protein level of FGF21 in the circulation

(A) Reverse-transcription PCR examination of FGF21 mRNA levels using liver samples collected from mice. (B) Quantitative determination of FGF21 mRNA levels using qPCR at major organs. (C) Representative images of green fluorescence and FGF21 IHC staining of the mouse liver. (D) Hydrodynamic injection of FGF21 gene generated persistent high level of circulating FGF21. Samples in (A)-(C) were collected 3 days after hydrodynamic injection. Values in (B) and (D) represent average ± SD (n = 5). ** $P < 0.01$ compared with control mice.

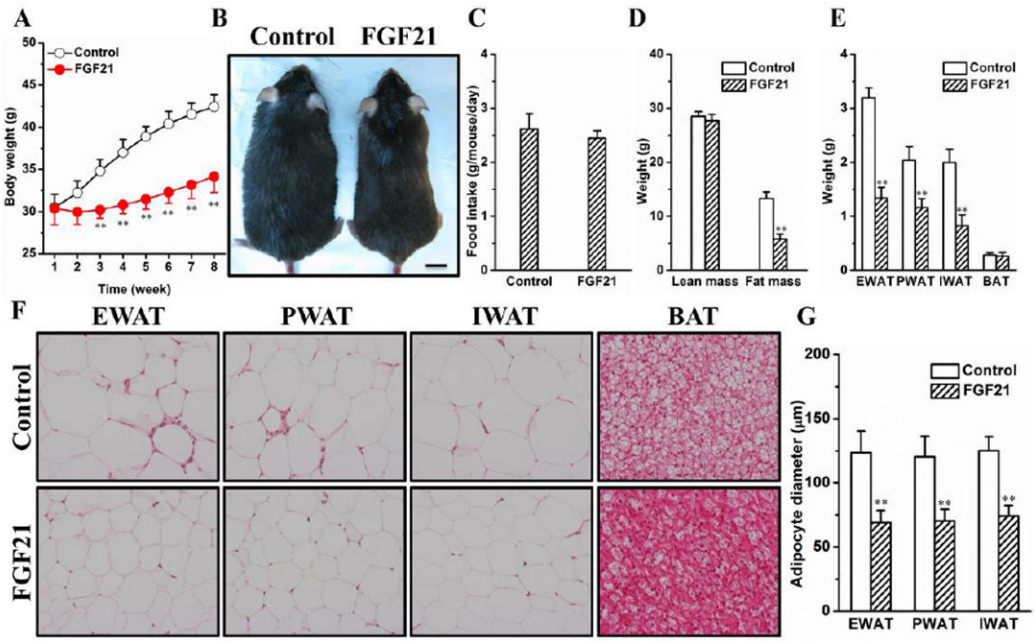

Figure 2. FGF21 gene transfer blocked HFD-induced adiposity and enlargement of adipocytes

(A) Growth curve. (B) Representative images of mice at end of the experiment (Bar length = 1 cm). (C) Food intake. (D) Body composition. (E) Weight of fat pad. (F) Representative images of H&E staining of adipose tissues. (G) Average diameters of adipocytes. Values in (A), (D) and (E) represent average ± SD (n = 5). Values in (G) represent average ± SD of total number of adipocytes seen in five tissue slices (50 adipocytes per slice). ** $P < 0.01$ compared with control mice.

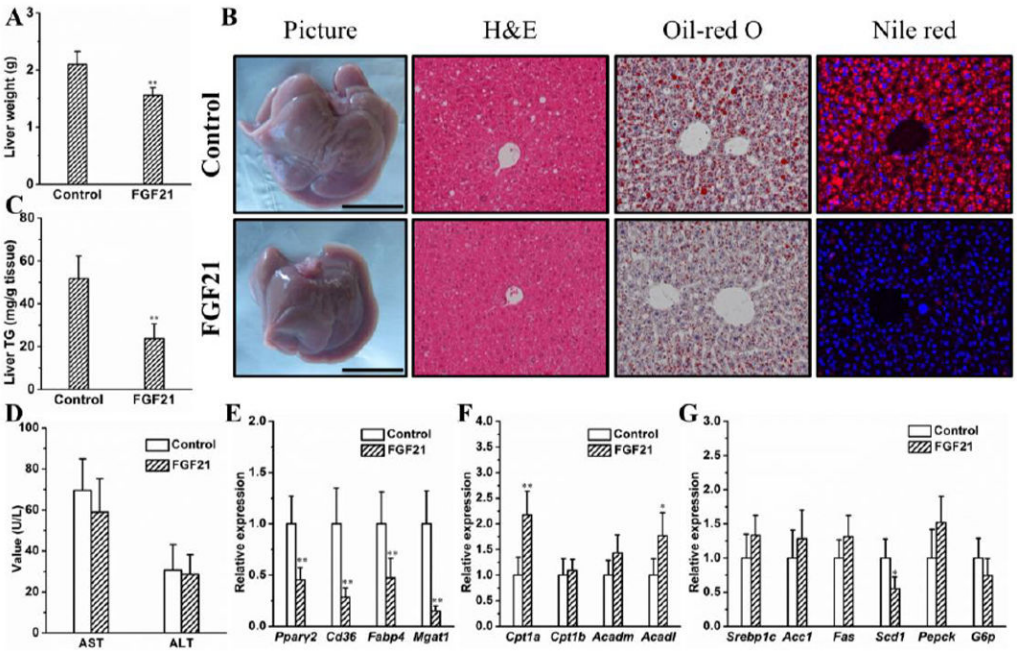

Figure 3. FGF21 gene transfer protected mice from HFD-induced fatty liver

(A) Liver weight. (B) Representative images of liver histological examinations (Bar length = 1 cm). (C) Liver triglyceride. (D) Blood concentration of aspartate aminotransferase and alanine aminotransferase in mice at the end of 8-week feeding period. (E), (F) and (G) Relative mRNA levels of key genes involved in lipid and glucose metabolism in the liver. Values in (A), (C) and (D)-(G) represent average ± SD (n = 5). * $P < 0.05$ compared with control mice, ** $P < 0.01$ compared with control mice.

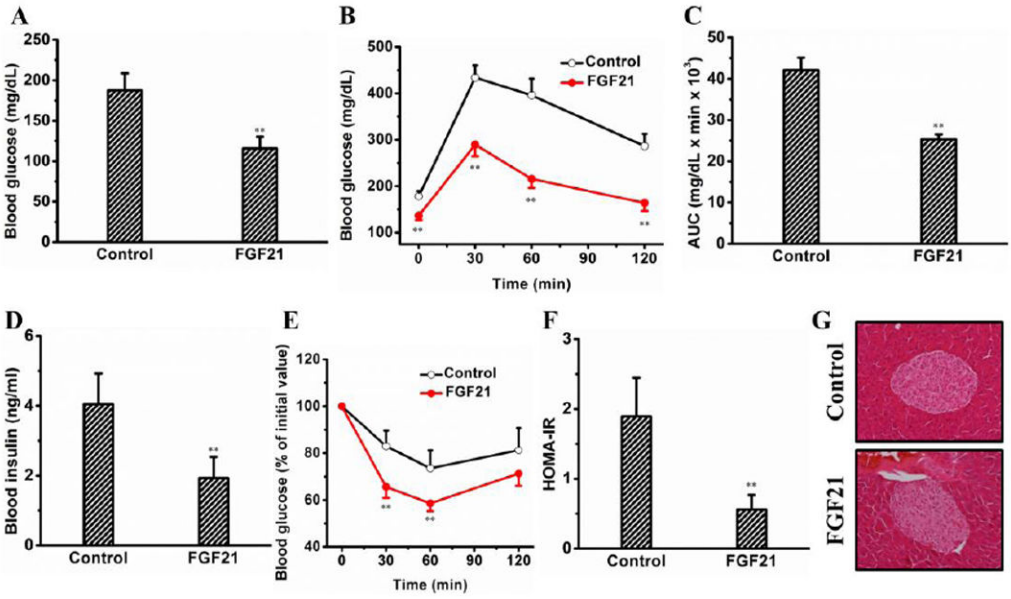

Figure 4. FGF21 gene transfer prevented HFD-induced insulin resistance and glucose intolerance

(A) Blood glucose. (B) Profiles of blood glucose concentration as function of time upon intraperitoneal injection of glucose. (C) Area under the curve of IPGTT. (D) Blood insulin. (E) Profiles of glucose concentration (percentage of initial value) as a function of time upon intraperitoneal injection of insulin. (F) Results of HOMA-IR analysis for insulin resistance. (G) Representative images from the H&E staining of the pancreas. Values in (A)-(E) represent average ± SD (n = 5). ** $P < 0.01$ compared with control mice.

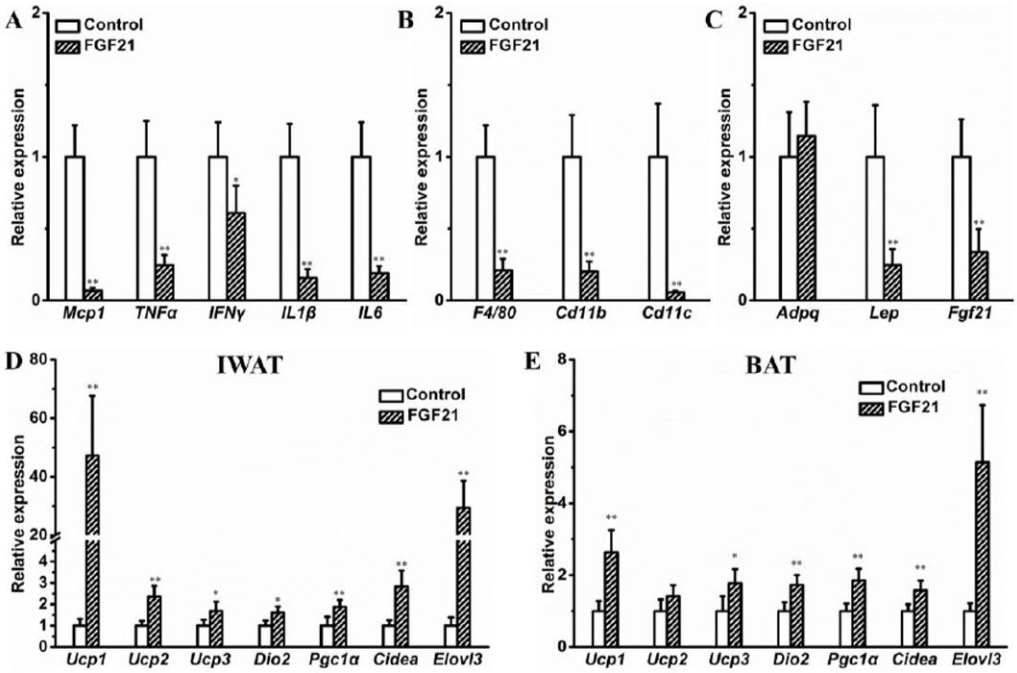

Figure 5. FGF21 gene transfer altered expression of genes in adipose tissues

(A) Relative mRNA levels of genes involved in chronic inflammation. (B) Relative mRNA levels of macrophage marker genes. (C) Relative mRNA levels of key adipokines. Relative mRNA levels of thermogenic genes in inguinal white adipose tissue (D) and brown adipose tissue (E). Values in (A)-(D) represent average ± SD (n = 5). * $P < 0.05$ compared with control mice, ** $P < 0.01$ compared with control mice.

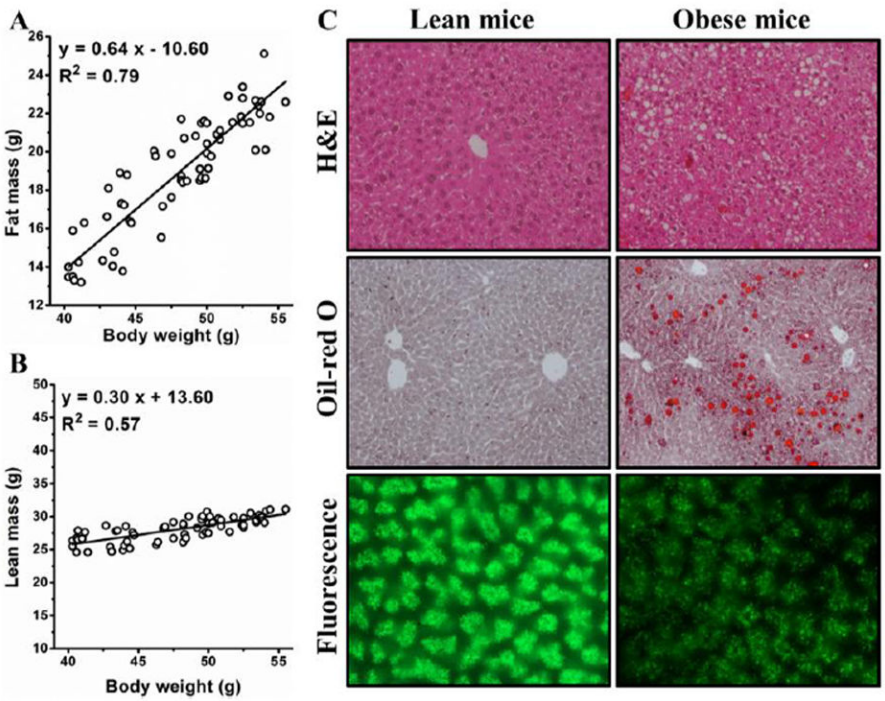

Figure 6. Adjustment of hydrodynamic tail vein injection in HFD-induced obese mice

The correlation of body weight to fat mass (A) and lean mass (B) in HFD-induced obese mice showed that fat mass provided a larger contribution to increase of body weight in obese mice. Values in (A) and (B) were collected from 64 obese mice. (C) Representative images of liver slice after hydrodynamic injection of GFP gene in lean mice and obese mice.

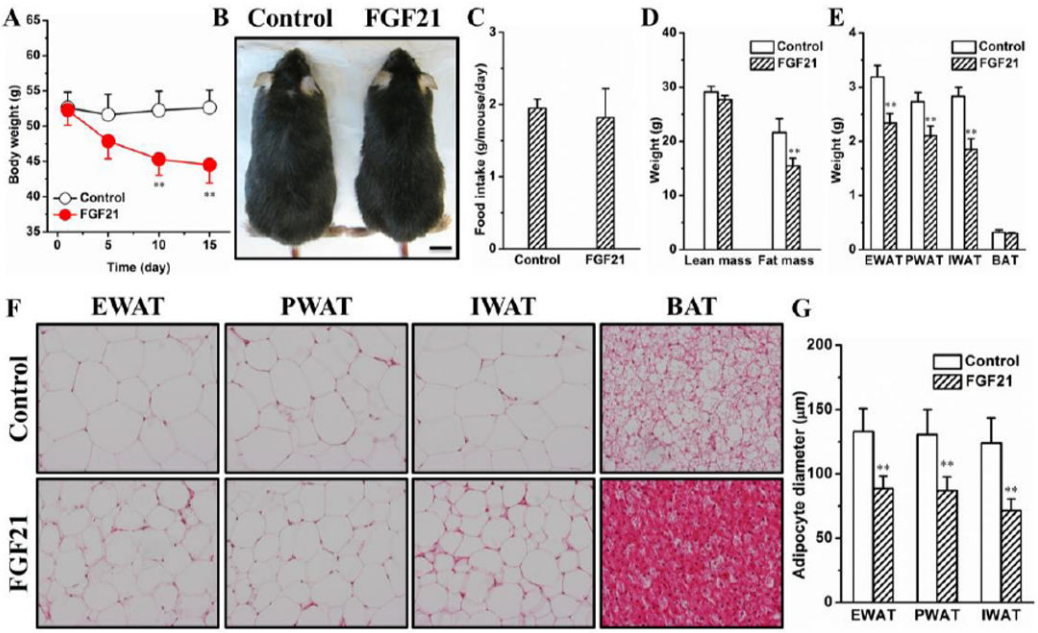

Figure 7. FGF21 gene transfer decreased body weight and reduced adipocyte size in HFD-induced obese mice

(A) Body weight change. (B) Representative images of mice at end of the experiment (Bar length = 1 cm). (C) Food intake. (D) Body composition analysis. (E) Weight of fat pad. (F) Representative images of H&E staining of adipose tissues. (G) Diameters of adipocytes. Values in (A), (D) and (E) represent average ± SD (n = 5). Values in (G) represent average ± SD of total number of adipocytes seen in five tissue slices (50 adipocytes per slice). ** $P <$ 0.01 compared with control mice.

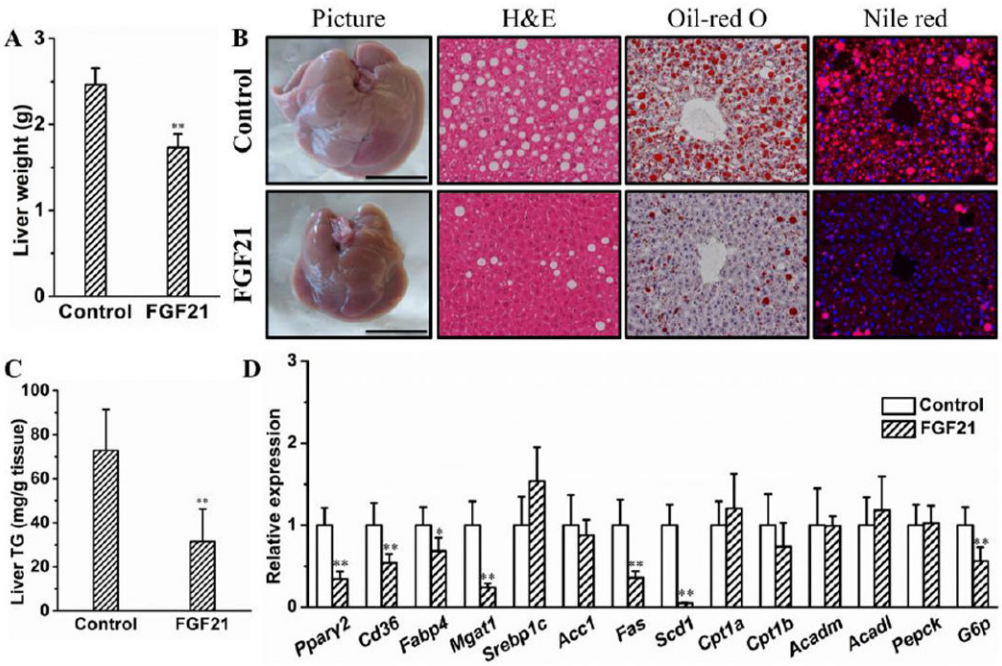

Figure 8. FGF21 gene transfer alleviated fatty liver in HFD-induced obese mice

(A) Liver weight. (B) Representative images of liver histological examinations (Bar length = 1 cm). (C) Liver triglyceride. (D) Relative mRNA levels of genes involved in lipids and glucose metabolism in the liver. Values in (A), (C) and (D) represent average ± SD (n = 5). * $P < 0.05$ compared with control mice, ** $P < 0.01$ compared with control mice.

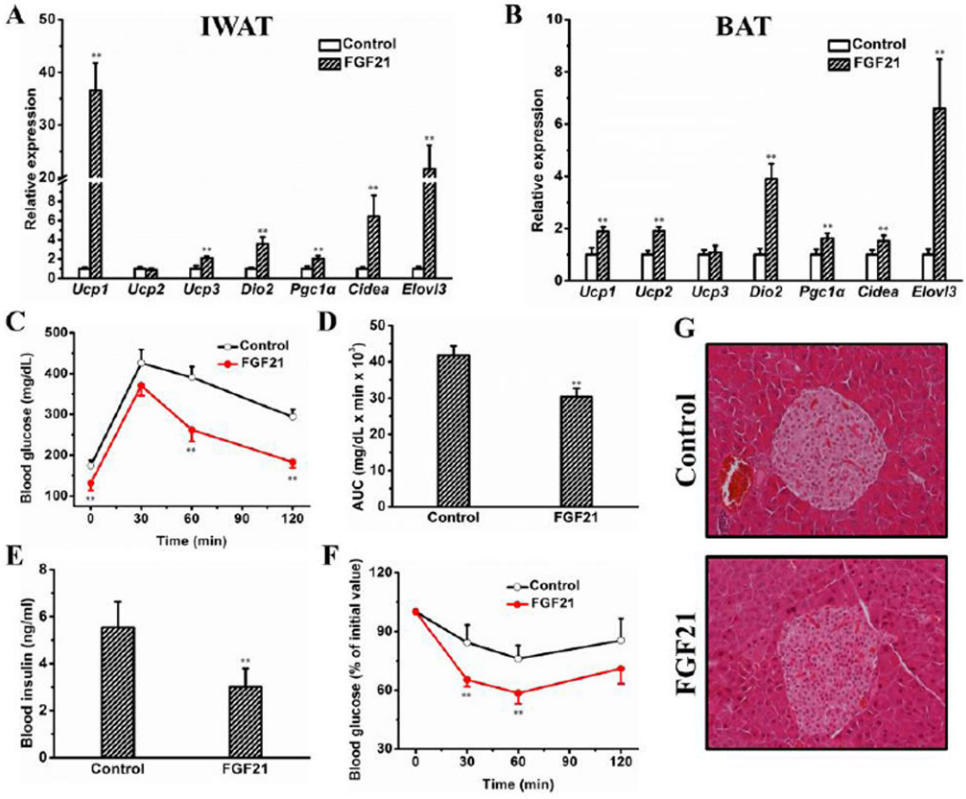

Figure 9. FGF21 gene transfer in HFD-induced obese mice altered gene expression in adipose tissues and improved glucose metabolism

FGF21 gene transfer increased expression of thermogenic gene in inguinal white adipose tissue (A) and brown adipose tissue (B). (C) Profiles of blood glucose concentration as function of time upon intraperitoneal injection of glucose. (D) Area under the curve of IPGTT. (E) Blood insulin. (F) Profiles of glucose concentration (percentage of initial value) as a function of time upon intraperitoneal injection of insulin. (G) Representative images from the H&E staining of the pancreas. Values in (A)-(E) represent average ± SD (n = 5). ** $P < 0.01$ compared with control mice.

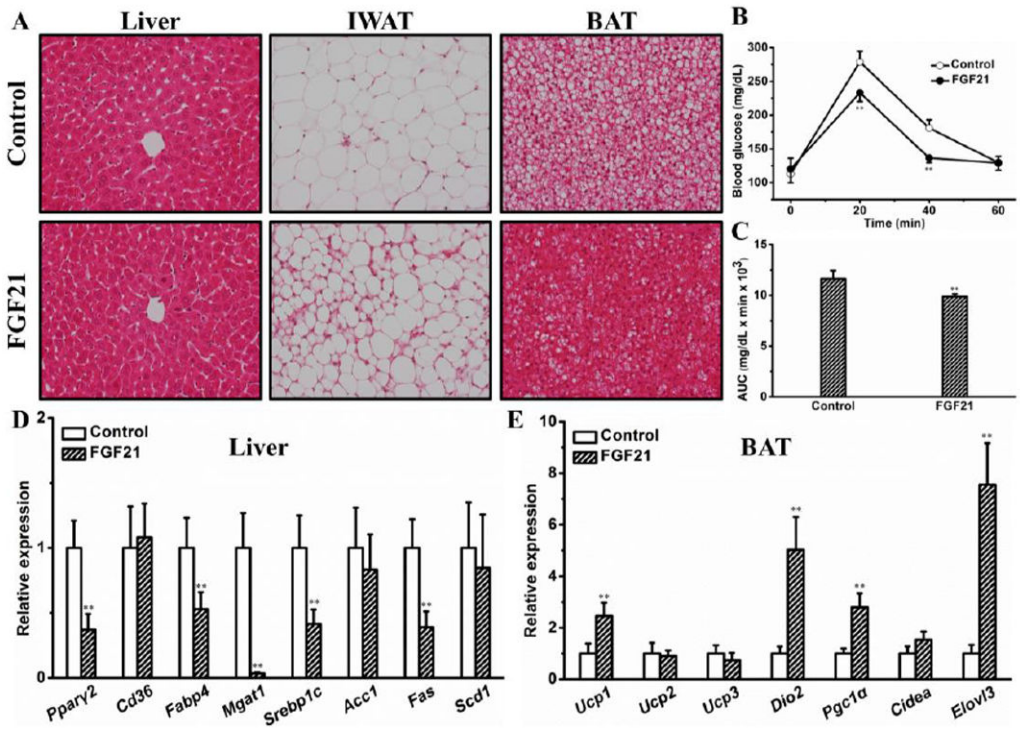

Figure 10. Acute effects of FGF21 gene transfer in lean mice

(A) Representative images of H&E staining of liver, inguinal white adipose tissue and brown adipose tissue. (B) Profiles of blood glucose concentration as function of time upon intraperitoneal injection of glucose. (C) Area under the curve of IPGTT. (D) Relative mRNA levels of key genes for lipogenesis in the liver. (E) Relative mRNA levels of thermogenic genes in brown adipose tissue. Samples were collected 7 days after injection. Values in (B)-(E) represent average ± SD (n = 5). ** $P < 0.01$ compared with control mice.